JOURNAL OF CATALYSIS 69, 345–358 (1981)

The Electronic Effect in Alloy Chemisorption: CO and H_2 Studies on Nickel Titanium Alloys

T. E. FISCHER, S. R. KELEMEN, AND R. S. POLIZZOTTI

Exxon Research and Engineering Company, P. O. Box 45, Linden, New Jersey 07036

Received September 26, 1980; revised January 26, 1981

This paper explores the electronic effect in alloys on chemisorption behavior with the examples of CO and H_2 adsorption on Ni/Ti alloys. A substantial ionic component in the chemical bonds of the alloy modifies the atoms from their elemental state. Chemisorption of H_2 shows that the compound does not possess the strong hydride formation tendency of titanium and adsorbs hydrogen in two states. CO adsorbs molecularly on Ni_3Ti at 150 K and near monolayer coverage a 3.4-eV splitting of the 5σ–1π-derived levels is obtained using ultraviolet photoemission spectroscopy. Dissociation of a portion of the CO occurs upon heating to 310 K accompanied by a decrease in splitting of the 5σ–1π levels to ~3.0 eV.

1. INTRODUCTION

Catalysis by alloys is an important current direction of research and development. Early attempts (*1, 2*) at modifying catalyst activity by alloying were guided by the rigid band model of the electronic structure of alloys (*3*); they sought to increase catalytic activity by tailoring the density of states at the Fermi level by alloying, for instance, copper to nickel.

We have come to know that the rigid band model is not correct for alloys such as Cu–Ni. Photoelectron spectroscopy (*4*) has confirmed the theoretical prediction (*5*) that the electronic structures of the nickel and copper atoms experience only subtle changes in the formation of an alloy. This appears to be true on the surface of the alloy as well as in the bulk (*6*).

The example of copper–nickel illustrates one important aspect of alloy catalysis, which Sachtler named the "ensemble effect" (*7*). If a surface reaction requires an active site consisting of a number of atoms of the active element arranged in a given order, (*8*) then the catalytic activity of the alloy is determined by the concentration of these active sites (or ensembles) on its surface.

The present work examines the other extreme case, namely, the electronic effect in alloy catalysis. Nickel–titanium alloys are known to form intermetallic compounds with large negative heats of formation. A previous study (*9*) of the compound Ni_3Ti revealed that electronic modification of the Ti and Ni atoms due to alloying is strong: the electronic and chemical character of the Ti and Ni is very different from what it is in the elemental metals. Ti can be described as being in the formal Ti^{3+} state and nickel in the Ni^- form. The overall electronic structure of the compound is qualitatively similar to that of iron in the sense of presenting an approximately half-filled band. However, Ni_3Ti differs from Fe in that the filled portion of the s–p–d band is located on the Ni atoms and the empty portion (electron acceptor) on the Ti atom.

A further difference between the Ni–Cu and Ni_3Ti is the absence of the statistical "ensemble" effect because the Ni_3Ti compound is ordered; the surface is a periodic repetition of identical components, which in the present case, consist of Ni_3Ti "molecules." The intermetallic compound thus represents the other extreme case of alloy catalysis. It is a relatively pure case of the "electronic," or "ligand" (*7*) effect of alloying. In order to probe the chemical and catalytic properties of such alloys, we stud-

0021-9517/81/060345-14$02.00/0
Copyright © 1981 by Academic Press, Inc.
All rights of reproduction in any form reserved.

ied the interaction of carbon monoxide and hydrogen with the compound Ni_3Ti and with the dilute alloy 90 Ni–10 Ti which contains 90 at.% Ni and 10 at.% Ti.

2. EXPERIMENTAL

Auger electron spectra were gathered either in the customary differentiated form dN/dE by using a phase-sensitive detector, or as direct energy distributions $N(E)$ by electron counting with a multichannel analyzer. The latter mode allowed the use of low primary electron current (10^{-8} A) which minimizes electron bombardment damage. For desorption measurements the sample was positioned in front of the quadrupole mass spectrometer and the temperature of the sample was increased linearly with time. The heating rate was 25 K per second.

Ultraviolet photoemission spectroscopy (UPS) was performed by measuring the energy distribution of electrons emitted by the samples under irradiation with ultraviolet light from a differentially pumped rare gas resonance lamp. The energy distributions of the electrons were measured with a double-pass cylindrical mirror analyzer (Physical Electronics). The presence or absence of hydrogen contamination was monitored with UPS energy distributions since Auger spectroscopy is insensitive to this species.

Samples of the intermetallic compound Ni_3Ti and of a solid solution of 10% titanium in nickel were prepared from Marz grade nickel and titanium foils obtained from Materials Research Corporation. The samples were prepared by arc melting weighed amounts of the starting materials in an argon atmosphere. Homogeneity of the alloys was assured by repeated stirring and arc melting. Metallographic examination showed that both alloys were homogeneous and free of precipitates. A thin, flat sample of the 10 at.% titanium solid solution was formed by rolling the button to a thickness of 0.2 mm. The intermetallic compound Ni_3Ti could not be rolled because of the brittleness of the material. The Ni_3Ti samples were cut by electron discharge machining and they were mechanically polished before insertion into the vacuum chamber.

Both alloys contained significant amounts of sulfur, phosphorus, and oxygen bulk impurities. Prior to chemisorption studies, each sample underwent extensive cleaning treatments consisting of sputtering with argon ions at various sample temperatures up to 1000°C during a cumulative time of approximately 50 h. This procedure ensured the segregation of the impurities to the surface and their subsequent removal by ion bombardment. After this treatment, no surface impurities were detected by Auger electron spectroscopy.

UPS energy distributions from the clean Ni–Ti alloys are shown in Fig. 1. In the case of nickel, chemisorbed hydrogen and surface hydrides exhibit emission in UPS energy distributions between −4 and −6.5 eV (*10–13*) from the Fermi level. The hydride of titanium exhibits a strong peak at −5.0 eV (*10, 11*) and chemisorbed hydro-

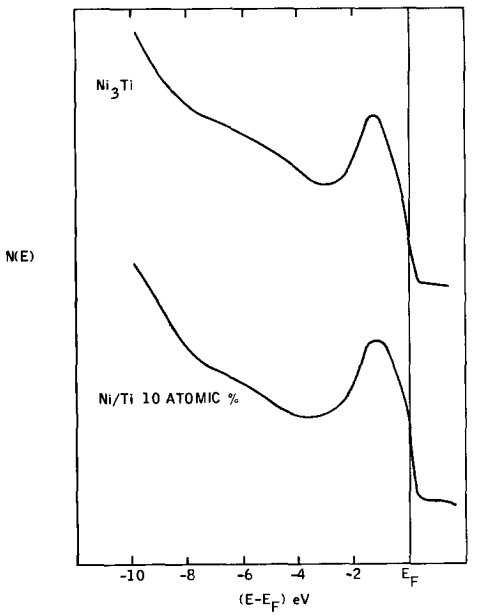

FIG. 1. Energy distributions of photoelectrons at $h\nu$ = 21.2 eV from clean polycrystalline Ni_3Ti and from a dilute alloy at 90% Ni–10% Ti.

gen on nickel at −6.0 eV (*12, 13*). We have assumed that the absence of strong emission in this energy region is indicative of minimal hydrogen contamination.

During a prolonged series of experiments that included heating to various temperatures, bulk impurities were observed to segregate to the surface and produce a broad peak centered at 6 eV below E_F in UPS energy distributions. The main impurities were sulfur for Ni_3Ti and oxygen for 90–10 Ni–Ti. The samples were cleaned anew when the surface concentration of these impurities exceeded 2% of the saturation concentration that could be obtained by deliberate adsorption of oxygen or decomposition of H_2S.

3. RESULTS

3.1 Hydrogen Adsorption on Ni_3Ti and 90 Ni–10 Ti

We investigated the adsorption of hydrogen on the intermetallic compound and the dilute alloy with the help of ultraviolet photoemission spectroscopy and temperature-programmed desorption. Both alloys showed that the bonding of hydrogen on the surface was different at low temperatures (T = 150 K) from those observed at and above room temperature. Figure 2A shows the UPS difference curves (i.e., the changes in electron energy distributions caused by hydrogen adsorption) obtained with He I radiation ($h\nu$ = 21.2 eV) after the clean Ni_3Ti surface held at 320 K was exposed to 10 Langmuirs of hydrogen. We observe a broad peak centered near 5.7 eV below the Fermi level; we also note a negative excursion of the difference curve within 2 eV from the Fermi level which corresponds to an attenuation of emission from the *d* band. By comparing the difference curve (2A) with the actual energy distributions, we find the adsorption of hydrogen causes a 6%

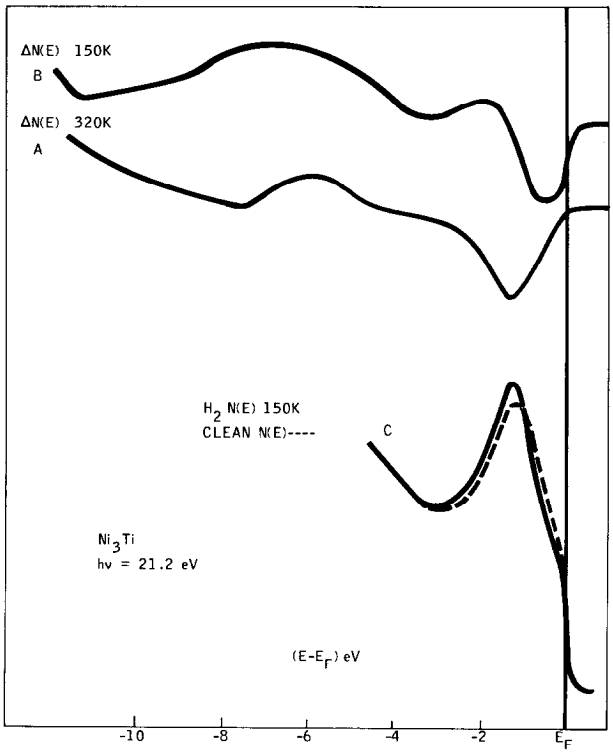

FIG. 2. Change in the energy distributions from Ni_3Ti due to 10 Langmuirs hydrogen exposure ($h\nu$ = 21.2 eV). Curve A: T = 320 K. Curve B: T = 150 K. Curve C: energy distributions $N(E)$ from the valence band of Ni_3Ti at 150 K showing the energy shift of the band upon exposure to H_2.

decrease in emission from the valence band. This decrease is uniform over the whole band within the limits of the noise.

The difference curve (2B) for 150 K is quite different. The peak attributed to the combination of hydrogen and metal orbitals is about 1 eV broader and is centered at 6.3 eV below E_F. The structure near the Fermi level consists of a sharp dip within 1 eV from E_F followed by a peak near -1.8 eV. This juxtaposition of a peak and valley in the difference curve represents the derivative of a peak and can indicate a shift of the peak on the energy scale. Comparison of the actual energy distributions (2C) reveals that hydrogen adsorption indeed causes a shift of 0.15 eV of the valence band toward higher binding energies with respect to the Fermi level. Another way of stating this result is that adsorption of hydrogen causes the Fermi level to rise by 0.15 eV in the valence band of the compound. At the same time, we find that emission from the valence band has increased by about 6%.

Similar behavior was observed with the dilute alloy as shown in Fig. 3. As with Ni_3Ti, we obtain a broad peak centered near -6.5 eV at 150 K, this peak sharpens and shifts to -5.7 eV at 320 K. The modification of the spectrum near the Fermi level amounts to a general decrease of emission from the d-band region at room temperature and a general increase of this emission at 200 K with a selective dip in an energy range at E_F that is narrower than that for Ni_3Ti. Such selective decrease is commonly observed in photoemission and is attributed to the downward shift in energy of metal orbitals and surface states involved in the chemisorption bond. An alternative interpretation in terms of a downward shift by 0.1 eV is again possible. We have heated this hydrogen-covered sample from 200 to 320 K. About half the

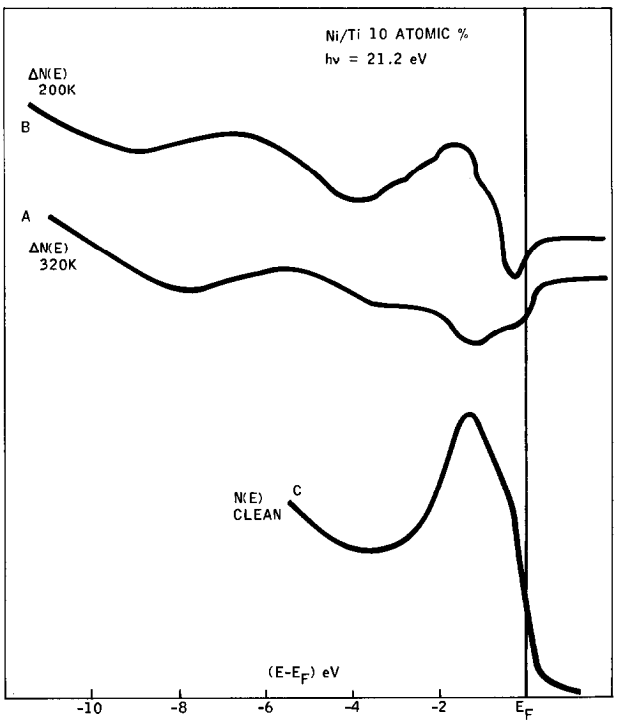

FIG. 3. Change in energy distributions of photoelectrons from 90 Ni–10 Ti upon 10 Langmuirs exposure to H_2. Curve A: T = 320 K. Curve B: T = 200 K. Curve C: energy distribution from the valence band of clean 90 Ni–10 Ti at 200 K.

hydrogen desorbed and the energy distributions and difference curves transformed to a shape similar to that of curve 3A: the hydrogen peak shifted to higher energies by 0.8 eV (becoming centered at −5.7 eV), the d band shifted upwards to assume the same position and shape as those for the clean surface, and d-band emission decreased by 10% to be ~4% weaker than that from the clean surface.

(Surface contamination from background gases prevented us from performing the slower inverse experiment of cooling a sample that had been exposed to hydrogen at 320 K.)

Figure 4 shows the flash desorption curves for hydrogen absorbed at near 150 K on the two alloys. The desorption peak for Ni_3Ti occurs at higher temperatures than for the dilute compound, pointing to a higher heat of desorption. By using second-order desorption kinetics

$$\frac{E_b}{RT_p^2} = \frac{n_0\nu_2}{b} e - \frac{E_b}{KT},$$

where E_b is the energy of desorption, T_p the temperature of the peak, n_0 the surface density of hydrogen atoms prior to desorption (assumed at 5×10^{14} cm^{-2}), b the heating rate (= 25 K sec^{-1}), and ν_2 the second-order desorption constant (assumed

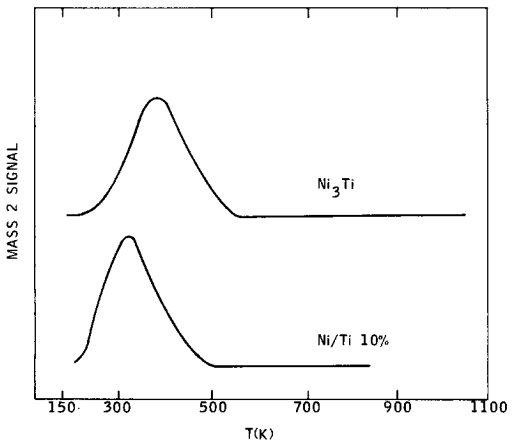

FIG. 4. Temperature-programmed desorption of hydrogen from Ni_3Ti and from the dilute alloy 90 Ni–10 Ti.

(*14*) at $\nu_2 = 8 \times 10^{-2}$ cm^2 sec^{-1}); we calculate from Fig. 4 a heat of desorption of 20 kcal/mole for hydrogen on the dilute alloy and 23.5 kcal/mole for Ni_3Ti.

3.2. CO on Ni_3Ti

Figure 5 shows the UPS difference curve obtained after the clean Ni_3Ti surface, held at 150 K, was exposed to 20 Langmuirs of CO. These curves were obtained at two different photon energies ($h\nu$ = 40.8 and 21.2 eV). The peak at −7.6 eV is assigned to the superimposed 1π and 5σ orbitals and the peak at −11.0 eV to the 4σ orbital of CO.

Figure 6 shows similar difference spectra obtained when the surface is heated in stages. The spectra labeled 130, 270, and 310 K were obtained after the surface had been heated to the indicated temperatures for 100 sec prior to obtaining the spectrum. The temperatures at which the spectra were measured are close to those indicated, except for the spectrum for 610 K which was measured during the cooling of the sample, near 400 K. These spectra were measured with the more intense He I radiation ($h\nu$ = 21.2 eV) to avoid possible surface contamination from background during the more lengthy measurements that would have been demanded by the He II radiation. At 130 K, we observe the same spectrum as in Fig. 5, namely, the 1π–5σ peak at $E - E_F$ = −7.6 eV. As the surface is heated to 270 K, the difference curve diminishes in amplitude, indicating that part of the CO has been desorbed, but the features of the spectrum have not been changed, i.e., the remaining CO is still adsorbed in molecular form with the 4σ-derived peak evident at −11 eV and the superimposed 1π–5σ peak at −7.6 eV.

At 310 K sample temperature, the features of the difference spectrum change. The peaks at −10.5 and 7.6 eV decrease in amplitude relative to the 270-K spectrum and a new peak appears at $E - E_F$ = −5.5 eV. Note also the change in the valence band emission. A sharp dip at −1.5 eV

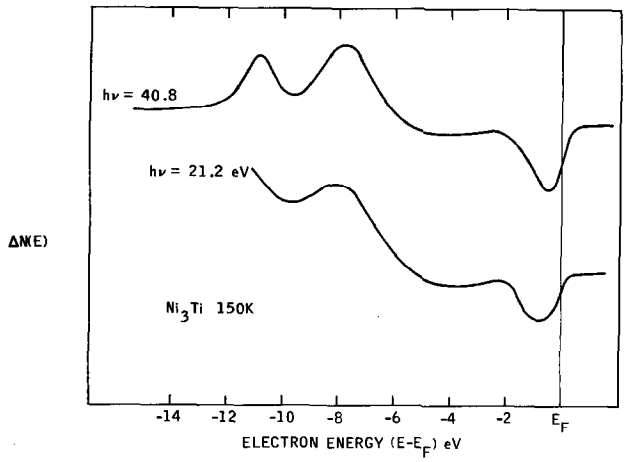

FIG. 5. Photoelectron energy distribution difference curve due to CO adsorption onto Ni_3Ti at T = 150 K. Photon energies as marked.

indicates that a different set of valence orbitals from the alloy are contributing in the bonding of the adsorbates. These changes indicate that a fraction of the adsorbate CO has dissociated with a portion remaining as molecular CO as evidenced by peaks at −10.5 and −7.6 eV.

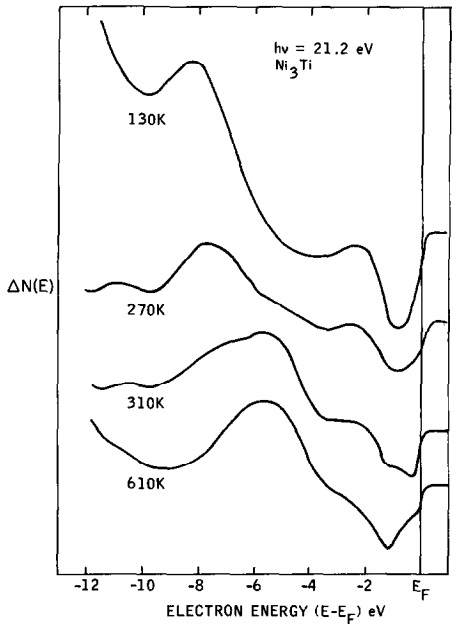

FIG. 6. Photoelectron energy distribution difference curves due to CO adsorption on Ni_3Ti at 130 K and heating to temperatures as marked for 100 sec. $h\nu$ = 21.2 eV.

At 610 K the difference spectrum consists of a prominent peak at −5.5 eV and a valence band emission decrease that shows a sharp peak at −1.5 eV. This difference curve is very similar to that obtained after exposure of this surface to oxygen. At this temperature all the adsorbed CO is dissociated. (Adsorption of carbon on this compound causes such small changes in the energy distributions of photoelectrons that the contribution of carbon to the difference curve at 610 K on Fig. 6 is negligible.)

When the clean Ni_3Ti surface at room temperature is incrementally exposed to CO gas, adsorption is dissociative at first (see Fig. 7, curve A); further CO is adsorbed in a molecular form (curve 7B). We estimate that on Ni_3Ti, roughly 40% of the CO adsorbed at room temperature is dissociated.

Adsorption with the surface at room temperature followed by flash desorption with a heating rate of 25 K sec^{-1} produces the mass 28 desorption spectrum shown in Fig. 8. The peak at 420 K results from the desorption of the molecular CO; recombination of the previously decomposed CO produces the desorption peak at 1000 K. Figure 9 shows the size of the carbon Auger peak obtained in an experiment in which Ni_3Ti was first cooled to 130 K and exposed

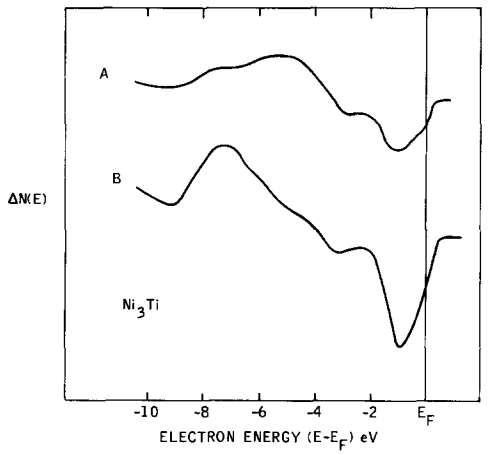

FIG. 7. Energy distribution difference curves due to CO adsorption on Ni_3Ti at room temperature. Curve A: change in distribution due to exposure to 1 Langmuir CO. Curve B: further change from curve A caused by CO saturation of the surface.

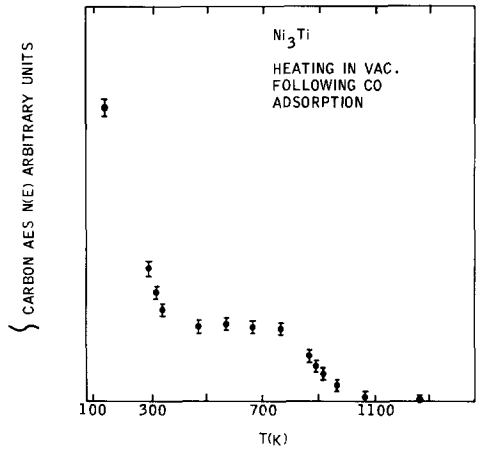

FIG. 9. Size of the carbon Auger peak following adsorption of CO on Ni_3Ti at 130 K and heating for 300 sec each to the temperatures shown.

to CO, then heated in stages under ultra-high vacuum. Heating time was 300 sec at each temperature plotted. At 130 K the shape of the carbon Auger peak was characteristic for CO molecules, as shown in Fig. 10A. Upon heating the sample to 370 K we observed a large decrease in the carbon Auger peak (Fig. 9); desorption of CO was simultaneously observed on the mass spectrometer. Between 370 and 775 K sample temperature, the carbon Auger peak size remained constant and the peak shape was that of a surface carbide (Fig. 10B) as a result of the dissociation of CO. When the sample temperature exceeded 775 K, the carbon Auger peak decreased and the residual gas analyzer detected evolution of CO molecules that we attribute to the recombination of the adsorbed carbon and oxygen. (This desorption of CO is observed at somewhat lower temperatures than in Fig. 8 because of the much smaller heating rate.) We also performed an experiment to probe the behavior of carbon adsorbed alone on Ni_3Ti. We exposed the clean Ni_3Ti surface to acetylene at room temperature. Heating the sample to 570 K caused dehydrogenation of the acetylene with the expected hydrogen evolution and carbidic Auger peak shape as in Fig. 10B. At sample temperatures exceeding 775 K, we observed a decrease in the carbon Auger peak without detecting gas evolution. Evidently, carbon dissolves in the Ni_3Ti bulk at these temperatures. These phenomena are more clearly displayed by the dilute Ni–Ti alloy and will be discussed in the following section.

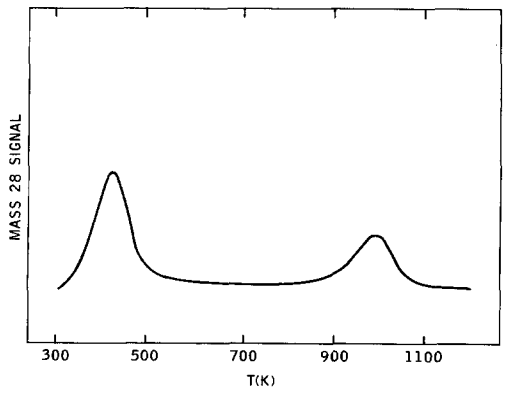

FIG. 8. Temperature-programmed desorption of CO from Ni_3Ti.

3.3 CO on 90 Ni–10 Ti

The flash desorption spectrum obtained after CO was adsorbed at low temperature on the dilute alloy is qualitatively similar to the one obtained with Ni_3Ti (Fig. 8) in that we observe two CO desorption peaks, one

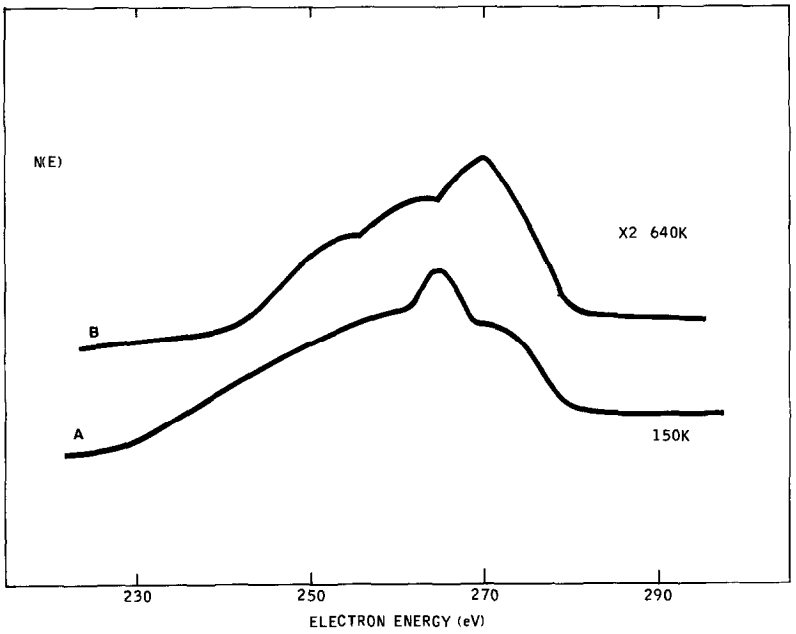

FIG. 10. Shape of the carbon Auger peak due to CO adsorption on Ni_3Ti. Curve A: T = 150 K, shape characteristic of CO. Curve B: T = 640 K, shape characteristic of a surface carbide.

below room temperature and another near 1000 K. Figure 11 compares the high-temperature desorption peaks of CO from the two alloys. The temperature-dependent Auger measurements (Fig. 12) reveal a somewhat different behavior than for the

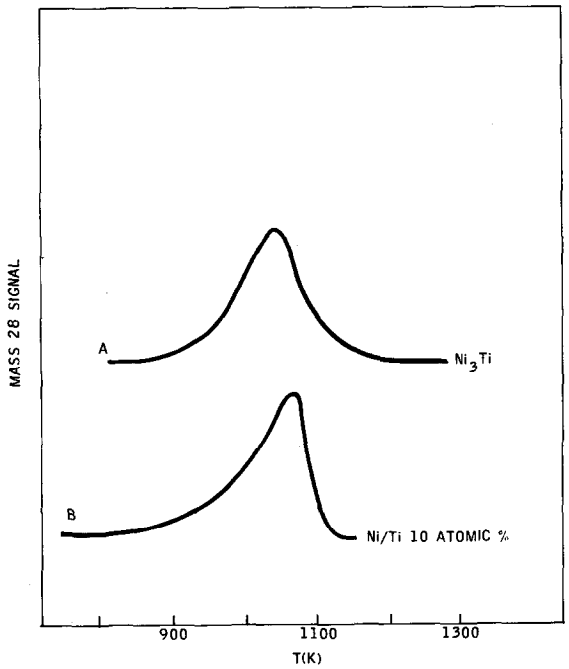

FIG. 11. High-temperature portion of temperature-programmed desorption of CO from Ni_3Ti and 90 Ni–10 Ti. The difference in shapes point to different controlling mechanisms.

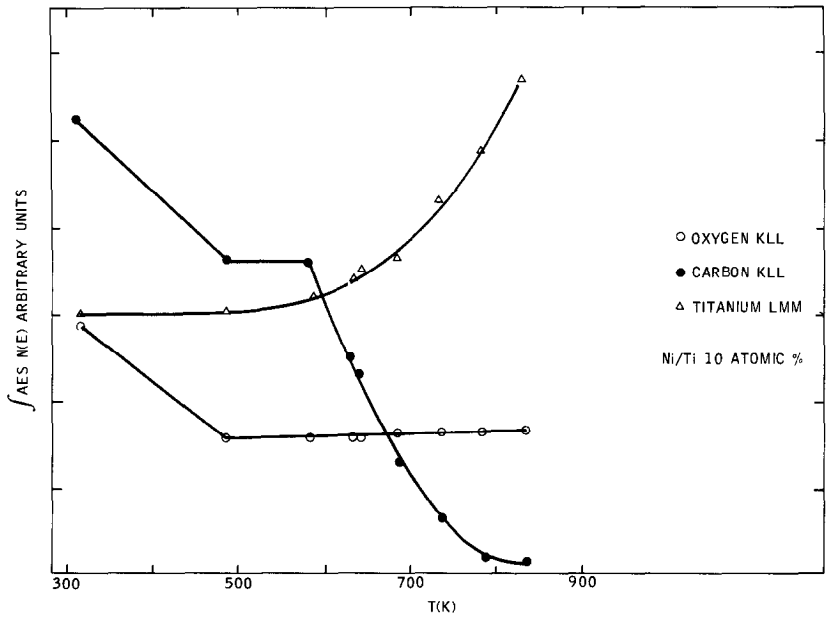

FIG. 12. Auger peak integrals for C, O, and Ti on 90 Ni–10 Ti after adsorption of CO at room temperature.

stoichiometric compound: we see a decrease of C and O signal showing desorption of molecular CO at $T < 470$ K followed by a plateau up to 570 K. The shape of the carbon Auger peak is again characteristic of a carbide above 470 K. At 570 K, the behavior of 90 Ni–10 Ti is now different from that of Ni_3Ti: the carbon Auger peak decreases while that of oxygen remains constant and the titanium peak increases. Carbon is dissolved in the bulk and the presence of oxygen "attracts" titanium to the surface. As the sample temperature reaches 1000 K, the residual gas analyzer detects the evolution of CO molecules from the sample, the oxygen Auger peak disappears, and the titanium peak decreases to the value it had before the adsorption experiment. These results are interpreted in terms of a recombination of oxygen with carbon migrating from the bulk to form CO which is desorbed.

Photoemission spectroscopy shows again the molecular adsorption of CO at low temperatures and its dissociation above 270 K. (These data are not shown because of their similarity with those of Fig. 3.) UPS data obtained at room temperature as a function of exposure to CO (Fig. 13) show that at first CO is dissociatively adsorbed after 0.5 Langmuir CO exposure (curve A) and shows a peak at $E - E_F = -6$ eV with the shape of the valence band emission dip near the Fermi level characteristic of dissociated CO as previously described for Ni_3Ti. Curve B shows the incremental change in energy distribution after exposure to another 0.5 Langmuir of CO. A small fraction of the additionally adsorbed gas is dissociated and the majority is molecularly adsorbed. Curve C shows that all additional CO is molecularly adsorbed by the peak at $E - E_F = -7.6$ eV which corresponds to the 5σ–1π peak of CO.

The following experiment shows that CO desorption at high temperatures indeed proceeds through diffusion of the dissolved carbon to the surface and its recombination with surface atoms. When we adsorb acetylene on the clean surface and heat the sample to 870 K, the acetylene is dehydrogenated and the carbon is dissolved in the

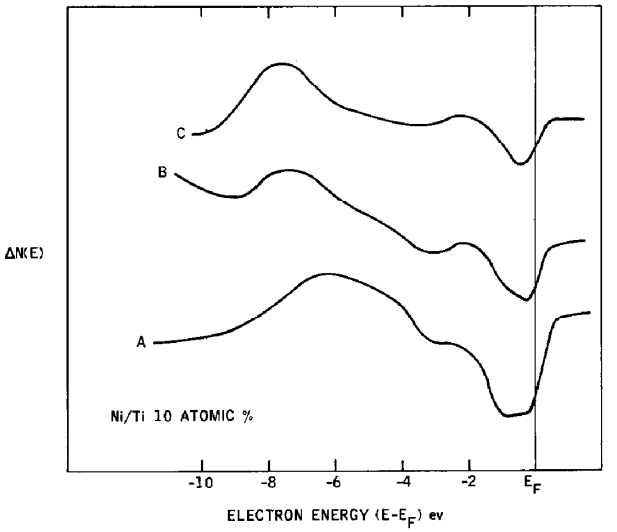

FIG. 13. Photoelectron energy distribution difference curves due to adsorption of CO onto 90 Ni–10 Ti at room temperature. Curve A: after exposure to initial 0.5 Langmuir of CO. Curve B: further difference induced by exposure to additional 0.5 Langmuir of CO after curve A. Curve C: difference induced after curve B by saturation with CO.

bulk. Subsequent adsorption of oxygen and heating to 1000 K leads to the formation and desorption of CO. In fact, as long as carbon is dissolved in the alloy, whatever its provenance, adsorption of oxygen and heating to 1000 K results in desorption of CO. Stable oxide layers are achieved after exhaustion of the dissolved carbon. This experiment can be repeated at least ten times before exhaustion of the bulk carbon occurs. Obviously, the concentration of native impurity carbon dissolved in the samples is much larger than the amount that is dissolved after CO dissociation. This explains why all the oxygen from the dissociated CO can be reacted away at high temperatures.

4. DISCUSSION

In this study we have attempted to address the question of the electronic effect in alloys by measuring chemisorption of H_2 and CO. There are three fundamental questions to be answered:

(1) To what extent is the behavior of Ni_3Ti similar to, or different from the sum of those of Ni and Ti?

(2) Are there adsorbate–surface interactions which are weak enough so that the adsorbate samples the chemical properties of the compound "molecule"?

(3) Are there adsorbate–substrate interactions which are so strong as to override the Ni–Ti bond and result in adsorbate–titanium or adsorbate–nickel interactions?

Pure titanium exhibits a strong tendency for hydride formation. Two separate UPS investigations have shown that titanium surfaces judged free of all impurities by Auger spectroscopy exhibited a peak at −5 eV in the energy distribution which is attributed to hydrogen (*10, 11*). In those studies it was impossible to prepare titanium surfaces free of all traces of hydrogen. In another study (*15*) it was concluded that when titanium is exposed to hydrogen, dissolution of hydrogen occurs and the latter evolves only after heating to elevated temperatures. The tendency of titanium to form bulk hydrides is further supported by a recent study of the interaction of deuterium with pure titanium films evaporated *in situ*, and titanium films with overlayers of carbon and oxygen. This study demonstrated

that titanium will form deuterides (*16*) despite the presence of carbon or oxygen overlayers.

Nickel, on the other hand, shows little tendency for hydride formation. Hydrogen is known to adsorb dissociatively on a clean nickel surface. The electronic structure of the hydrogen-covered surface, as measured by photoemission (*13, 17, 18*), changes as the temperature is raised from 200 to 300 K. Temperature-programmed desorption measurements (*14*) show that hydrogen recombines and desorbs below 420 K; a fraction of the gas desorbs below room temperature. Yamahaka and co-workers (*19*) have investigated the absorption properties of intermetallic compounds of titanium with Fe, Co, Ni, and Cu. They have found that Ti_3Ni and Ni–Ti readily react with large quantities of hydrogen to form hydrides; however, the intermetallic compound Ni_3Ti exhibits poor absorption behavior and no bulk adsorption of hydrogen.

The properties of hydrogen adsorbed on Ni_3Ti and on the dilute alloy are qualitatively similar to those of hydrogen on nickel in that hydrogen desorbs at relatively low temperatures ($T < 600$ K) and the electronic structure of the hydrogenated surface presents a low-temperature ($T = 200$ K) form that is different from the spectrum at room temperature and above. Angle-resolved photoemission measurements (*17*) have shown that a peak at 5.8 eV below the Fermi energy of hydrogen-covered nickel was not due to H-bonding levels, but to an enhancement of direct transitions from the bulk *s* band of Ni. A peak observed at 9 eV below E_F only at low temperatures (*18*) is attributed to an H-bonding orbital. It is possible that our spectra represent a similar situation since we see a peak at 5.7 eV below the Fermi energy at room temperature and a broad peak at 150 K that could be considered as the superposition of two peaks, at 5.7 eV and at 8 eV below E_F. Such an interpretation would be supported by the fact that cluster model calculations (*9*) resulted in and *s–d* level at the appropriate energy for Ni_4 and for Ni_3Ti. A positive identification of these features would of course require angle-resolved measurements on single crystals.

At low temperature, we have pointed out that the modification of the emission from the *d* band is also compatible with an increase in emission and a rise in the Fermi level in the bands. This interpretation could point toward a charge transfer from the adsorbed hydrogen to the empty *d* orbitals of the metal.

The fact that about half the adsorbed hydrogen is desorbed and the remainder transforms to the high-temperature form as the hydrogen-covered surface is heated from 200 to 320 K suggests that the low-temperature form is a weakly bound precursor and that adsorption into the more strongly chemisorbed form is activated. Unfortunately, the critical experiment of irreversibility of the high-temperature form upon cooling could not be performed because of complications from possible contamination from the background.

The flash desorption spectra (Fig. 4) show that the bonding of hydrogen is somewhat stronger on Ni_3Ti than on the dilute Ni–Ti alloy. Desorption of hydrogen extends to about 560 K on Ni_3Ti, to 500 K on 90 Ni–10 Ti; it is completed at 420 K on nickel under similar conditions (*12, 14*). This implies that the alloying of nickel with titanium increases the hydrogen bond strength, but does not create any sites that bond hydrogen strongly enough to cause desorption at temperatures as high as 1000 K as on titanium. We can summarize our results with hydrogen adsorption as follows: the alloying of relatively small amounts (10 and 25%) of titanium to nickel does not produce a mixture of surface sites with the adsorption properties of the two elements but produces a distinct material whose properties are qualitatively similar to those of nickel. The addition of titanium causes a shift of the hydrogen-bonding orbitals in the electronic structure and an increase in the de-

sorption energy of hydrogen. The interaction of the hydrogen with the alloy is too weak to override the Ni–Ti interaction within the metal.

Our experiments show that CO is adsorbed exclusively in molecular form at low temperature. Both Ni–Ti alloys dissociate about 40% of the total amount of CO, that will adsorb at room temperature, which is approximately 20% of the total amount adsorbed at 150 K. Titanium is known to adsorb CO in dissociated form at room temperature (*20–24*). On low-index surfaces of nickel CO is adsorbed in molecular form at all temperatures (*20, 23–25*). Stepped and irregular surfaces of nickel adsorb CO molecularly at room temperature and upon heating, they dissociate 6 to 10% of the adsorbed CO (*26*), the remainder desorbs without dissociation. The behavior of the Ni/Ti alloys is thus intermediate between those of the constituent metals.

Broden and co-workers (*27*) have surveyed CO adsorption on transition metals and found that the tendency of these metals to dissociate CO increases as one moves upwards and to the left in the periodic table. They were able to correlate the magnitude of the splitting between the 4σ and 1π orbitals of adsorbed CO with the subsequent dissociation of the adsorbed molecule at higher temperatures. This correlation was again observed on iron, where the $4\sigma-1\pi$ splitting of CO was 3.0 eV on the clean Fe(110) surface and 3.6 eV on the surface covered with potassium which promotes CO decomposition (*28, 29*). On the other hand the $4\sigma-1\pi$ splitting on six reported Ni surfaces ranged between 3.0 and 3.2 (*27*). Our observation of $4\sigma-1\pi$ splitting of 3.4 eV where CO is adsorbed on Ni_3Ti as 150 K indicates a tendency for the Ni_3Ti surface to act as a CO dissociation catalyst.

The increase of the $4\sigma-1\pi$ splitting of CO adsorbed on metals, as compared to the splitting of 2.75 eV in the gas phase has been attributed (*27, 29–31*) to a donation of metal electrons to the antibonding $2\pi^*$ of adsorbed CO. This increases the C–O distance, reduces the overlap of the atomic orbitals, and increases the energy of the strongly bonding 1π orbital more than that of the 5σ orbital.

There appear at first glance to be two plausible reasons for CO dissociation activity: (1) the electronic structure of Ni_3Ti, being similar to that of iron, allows the transfer of electronic charge to the CO antibonding orbital with reasonably low activation energy, and (2) the high affinity of Ti for oxygen causes the breaking of C–O and Ti–Ni bonds and the formation of a Ti–O surface complex. According to the former explanation, the behavior of the adsorbing CO is determined by the properties of the Ni_3Ti "molecule"; the second explanation, on the contrary, implies that the strong interaction of the titanium atoms with oxygen is determining and that its alloying with nickel is not as important.

The fact that we observe the large $5\sigma-1\pi$ splitting of 3.4 eV for CO adsorbed on Ni_3Ti at 150 K signifies a strong electronic interaction of the adsorbate with Ni_3Ti and favors explanation (1). At 270 K, we observe the coexistence of CO dissociation products and molecular CO; the latter shows a reduced $5\sigma-1\pi$ splitting of 3.0 eV. Evidently, the surface properties of Ni_3Ti are modified by the adsorption of C and O in such a way as to reduce the electronic interaction of the substrate with the CO molecules. Explanation (2) thus appears more appropriate for the consequences rather than the cause of CO dissociation.

The interaction of the alloys with oxygen (either from O_2 gas or from CO dissociation) can cause CO dissociation poisoning and the reduction in the $5\sigma-1\pi$ energy split to ~3.0 eV of the remainder of the molecular CO adsorbed on Ni_3Ti at 310 K and provides good evidence that the oxygen interaction with the titanium atoms is sufficiently strong to override the Ti–Ni complex.

5. CONCLUSION

The purpose of this investigation has been to explore the electronic, or ligand, effect in alloys exhibited in chemisorption. We have chosen the compound Ni_3Ti and the dilute alloy containing 10% titanium in nickel because the large negative heat of formation of the compound had suggested and a previous investigation had confirmed (*9*) that enough of an ionic and covalent component exists in the Ni–Ti bond to alter the electronic and chemical properties of Ni and Ti sites on the surface with respect to those of elemental nickel and titanium. The surface chemical properties were probed by the adsorption of hydrogen and carbon monoxide.

With respect to the adsorption of hydrogen, the two alloys behave similarly to nickel in that hydrogen is adsorbed dissociatively in two electronically different states, one at low (<200 K) temperature and the other at room temperature and above. They differ from titanium in that desorption of hydrogen at high temperatures is not observed with the two alloys. Quantitative effects of alloying Ti to Ni are a different position of the hydrogen-bonding levels with respect to the Fermi level and an increase (from 20 to 23.4 kcal/mole) of the desorption energy of hydrogen. The hydrogen gas thus does not experience the atomic properties of Ni and Ti on the surface, but interacts with the Ni_3Ti compound.

CO adsorbs in molecular form at low temperatures but the relatively large splitting (3.4 eV) between the 4σ- and 1π-derived levels of the adsorbed molecule on Ni_3Ti points to a greater tendency of the alloy to subsequently dissociate CO at room temperature where 40% of the CO as observed is dissociated. At higher temperatures carbon diffuses into the bulk near 600 K on the dilute alloy and 775 K on Ni_3Ti. The oxygen remaining on the surface causes segregation of Ti on the dilute alloy only. At higher temperatures (900 K when the heating rate is 25 K/sec), the dissolved carbon recombines with the oxygen and desorbs. The facts that oxygen causes surface segregation of Ti in the dilute alloy and decreases the 4σ–1π splitting of CO on the Ni_3Ti compound are interpreted as evidence that oxygen overrides the Ti–Ni bonds and interacts preferentially with Ti atoms. The 3.4-eV splitting between the 4σ and 1π levels of CO chemisorbed at low temperature indicates that the CO molecule interacts with the Ni_3Ti compound.

ACKNOWLEDGMENTS

The authors are indebted to T. M. Pugel and F. K. King for their experimental assistance throughout the course of this work, and J. A. Schwarz for helpful discussions.

REFERENCES

1. Reynolds, P. W., *J. Chem. Soc. London*, 265 (1950).
2. Charpurey, M. K., and Emmett, P. H., *J. Phys. Chem.* **65**, 1182 (1962).
3. Mott, N. F., and Jones, H., "Properties of Metals and Alloys." Oxford Univ. Press, London, 1936.
4. Seib, D. H., and Spicer, W. E., *Phys. Rev. B* **2**, 1676 and 1694 (1970).
5. Lang, N. D., and Ehrenreich, H., *Phys. Rev.* **168**, 605 (1968).
6. Yu, K. Y., Helms, C. R., Spicer, W. E., and Chye, P. W., *Phys. Rev. B* **15**, 1629 (1977).
7. Van Santen, R. A., and Sachtler, W. M. H., *in* "Advances in Catalysis and Related Subjects," Vol. 26, p. 69. Academic Press, New York/London, 1977.
8. Balandin, A. A., *Z. Phys. Chem.* **132**, 289 (1929).
9. Fischer, T. E., Kelemen, S. R., Wang, K. P., and Johnson, K. H., *Phys. Rev. B* **20**, 3124 (1979).
10. Eastman, D. E., *Solid State Commun.* **10**, 933 (1972).
11. Hagstrom, A. L., Johansson, L. I., Hagstrom, S. B. M., and Christensen, A. N., *J. Electron Spectro. Relat. Phenom.* **11**, 75 (1977).
12. Conrad, H., Ertl, G., and Latta, E. E., *Surface Sci.* **58**, 578 (1976).
13. Demuth, J. E., *Surface Sci.* **65**, 369 (1977) and references therein.
14. Goodman, D. W., Yates, J. T., and Madey, T. E., *Surface Sci.* **93**, L135 (1980).
15. Schwarz, J. A., Polizzotti, R. S., and Burton, J. J., *Surface Sci.* **67**, 10 (1977).
16. Malinowski, M. E., *J. Vac. Sci. Technol.* **15**, 39 (1978).

17. Himpsel, F. J., Knapp, J. A., and Eastman, D. E., *Phys. Rev. B* **19**, 2872 (1979).
18. Eberhardt, W., Greuter, F., and Plummer, E. W., submitted for publication.
19. Yamahaka, K., Saito, H., and Someno, M., *Nippon Kagaku Kaishi* **8**, 1267 (1976).
20. Hooker, M. P., and Grant, J. T., *Surface Sci.* **62**, 21 (1977).
21. Eastman, D. E., *Solid State Commun.* **10**, 933 (1972).
22. Polizzotti, R. S., unpublished.
23. Doyner, R. W., and Roberts, M. W., *J. Chem. Soc. Faraday Trans. I* **70**, 1819 (1974).
24. Christmann, K., Schober, O., and Ertl, G., *J. Chem. Phys.* **60**, 4719 (1974).
25. Eastman, D. E., Demuth, J. E., and Baker, J. M., *J. Vac. Sci. Technol.* **11**, 273 (1974).
26. Erly, W., and Wagner, H., *Surface Sci.* **74**, 333 (1978).
27. Broden, G., Rhodin, T. N., Brucker, C. F., Benbow, R., and Hurych, Z., *Surface Sci.* **59**, 593 (1976) and references therein.
28. Broden, G., Gafner, G., and Bonzel, H. P., *Appl. Phys.* **13**, 333 (1977).
29. Broden, G., Gafner, G., and Bonzel, H. P., *Surface Sci.* **84**, 295 (1979).
30. Rhodin, T. N., and Brucker, C. F., *Solid State Commun.* **23**, 275 (1977).
31. Brucker, C. F., and Rhodin, T. N., *Surface Sci.* **86**, 638 (1979).